Robust Control of Belt Drive System with Backlash and Friction

M2017SC013 Kenji YOSHIDA
supervisor : Isao TAKAMI

1 INTRODUCTION

A belt drive device is currently being put to practical use in machine tools such as belt conveyors and CVTs which are the transmission equipment in automobiles. This device uses a toothed belt to transmit the force between the gears to rotate the load by the drive motor. The purpose of this paper is to maintain the control performance by appropriately responding to the factors that degrade the control performance in positioning control of the belt drive system. The following three factors are considered as factors deteriorating of control performance in the belt drive device. The first is the backlash caused by the gap between the belt and the tooth attached to the shaft and the elastic deformation of the tooth. A transmission delay occurs by the backlash. By this effect, positioning deteriorates, which may cause limit cycles and steady-state deviations. The second is the effect of friction between the shaft and the bearing of motor. Due to this, the accuracy of positioning may deteriorate. The third is the uncertainty that exists in the dynamic characteristics of the system. The fluctuation of the moment of inertia of the load disc and the drive disc can be raised. There is a possibility that response delay and instability of the system may be caused by this. In this paper, we propose a positioning control system design method for a belt drive device in which the above three problems simultaneously exist. For the nonlinear friction, the LuGre model is linearized, and the control system is designed by applying the linear control theory. Based on the dead zone model [1], the backlash is regarded as a disturbance, and the model of the controlled object is represented by a linear system. In addition, we introduce a servo system into state equations using matrix polytope representation for varying parameters. Next, a control system that guarantees robust stability with respect to the fluctuation parameter is constructed based on the H_∞ control theory. The effectiveness of the proposed method is shown from comparison with other control system design method.

2 MODELING

2.1 Modeling of Belt Drive System

A schematic diagram of the belt drive system used in this paper is shown in Figure 1. Further, physical parameters of the system are shown in Table 1.

Let θ_d be the angle of the drive disk, $\dot{\theta}_d$ be its velocity, and F_d be the nonlinear friction. Let two forces working between the drive disc and the idler pulley be F_1, F_2 respectively. From Figure 1, the motion equation of the drive disk is obtained as follows;

$$J_d\ddot{\theta}_d(t) = \tau(t) + \{F_1(t) - F_2(t)\}r_d - c_d\dot{\theta}_d(t) - F_d. \quad (1)$$

Let θ_p be the angle of the idler pulley. Let two forces working between the load disk and the idler pulley be F_3, F_4 respectively. From Figure 1, the motion equation of idler pulley is obtained as follows;

$$J_p\ddot{\theta}_p(t) = \{F_2(t) - F_1(t)\}r_{pd} + \{F_4(t) - F_3(t)\}r_{pl}. \quad (2)$$

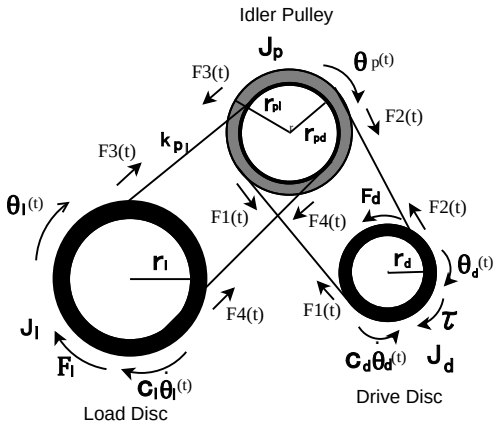

Figure 1 Schematic diagram of belt drive system

Table 1 Physical parameters

detail	character
Radius of Load Disc	r_l
Radius of Drive Disc	r_d
Radius of Bottom Pulley	r_{pd}
Radius of Top Pulley	r_{pl}
Moment of Drive Disc	J_d
Moment of Idler Pulley	J_p
Moment of Load Disc	J_l
Viscosity friction coefficient of Drive Disc	c_d
Viscosity friction coefficient of Load Disc	c_l
Gear ratio between drive disk and load disk	g_{dl}
Gear ratio between drive disk and Idler Pulley	g_{di}
Gear ratio between Idler Pulley and load disk	g_{il}
Input torque	τ

Let θ_l be the angle of the load disk, $\dot{\theta}_l$ be its velocity, and F_l be the nonlinear friction. From Figure 1, the motion equation of load disk is obtained as follows;

$$J_l\ddot{\theta}_l(t) = \{F_3(t) - F_4(t)\}r_l - c_l\dot{\theta}_l(t) - F_l. \quad (3)$$

In this modeling, the dynamical characteristics of the idler pulley are included in the dynamical characteristics of the drive disc. Furthermore, the tension was expressed using Hooke's law. The motion equations of the drive disk and the load disk taking these into account are expressed by the following equations,

$$\begin{aligned}\tau(t) &= J_d^*\ddot{\theta}_d(t) + c_d\dot{\theta}_d(t) + F_d \\ &\quad + g_{dl}^{-2}K_L\theta_d(t) - g_{dl}^{-1}K_L\theta_l(t) \quad (4)\\ 0 &= J_l\ddot{\theta}_l(t) + K_L\theta_l(t) - g_{dl}^{-1}K_L\theta_d(t) + c_l\dot{\theta}_l(t) + F_l. \quad (5)\end{aligned}$$

Here, J_d^* and K_L are defined as follows,

$$J_d^* \triangleq J_d + gr_{dl}^{-2}J_p \quad (6)$$

$$K_L \triangleq 2k_{pl}r_l^2. \quad (7)$$

2.2 Backlash Model

Backlash is the portion of the gap that is generated during engagement between the gear and the gear. This causes a delay of torque transmission. The backlash figure is shown in Figure 2.

Figure 2 Backlash

Belts generate transmission torque in Eq.(4) and Eq.(5). The transmission torque $T(t)$ is defined as follows,

$$T(t) := K_L\{g_{dl}^{-1}\theta_d(t) - \theta_l(t)\}. \tag{8}$$

By Eq.(8),Eq.(4) and Eq.(5) are given as follows,

$$J_d^*\ddot{\theta}_d(t) = \tau(t) - c_d\dot{\theta}_d(t) - F_d + g_{dl}^{-1}T(t) \tag{9}$$

$$J_l\ddot{\theta}_l(t) = -c_l\dot{\theta}_l(t) - F_l + T(t). \tag{10}$$

The backlash nonlinearity is represented by the dead zone model. The dead zone model is expressed as follows[1].

$$D_\alpha(t) = \begin{cases} g_{dl}^{-1}\theta_d - \theta_l - \alpha & (g_{dl}^{-1}\theta_d - \theta_l > \alpha) \\ 0 & (|g_{dl}^{-1}\theta_d - \theta_l| < \alpha) \\ g_{dl}^{-1}\theta_d - \theta_l + \alpha & (g_{dl}^{-1}\theta_d - \theta_l < -\alpha) \end{cases} \tag{11}$$

Here,α is the backlash angle. The transmission torque $T(t)$ is defined as follows,

$$T(t) = K_L D_\alpha(\theta_d(t), \theta_l(t)). \tag{12}$$

By Eq.(12), Eq.(11) is rewritten as follows,

$$D_\alpha = g_{dl}^{-1}\theta_d(t) - \theta_l(t) + d_\alpha(t). \tag{13}$$

Here,d_α is defined as follows,

$$d_\alpha(t) = \begin{cases} -\alpha & (g_{dl}^{-1}\theta_d - \theta_l > \alpha) \\ -g_{dl}^{-1}\theta_d + \theta_l & (|g_{dl}^{-1}\theta_d - \theta_l| < \alpha) \\ +\alpha & (g_{dl}^{-1}\theta_d - \theta_l < -\alpha), \end{cases} \tag{14}$$

where d_α is a backlash considered as a disturbance. By Eq.(11)-Eq.(14),the final motions equation of the belt drive system including backlash and friction is given by Eq.(15) and Eq.(16),

$$\begin{aligned} J_d^*\ddot{\theta}_d(t) &= \tau(t) - c_d\dot{\theta}_d(t) - F_d - K_L g_{dl}^{-2}\theta_d(t) \\ &\quad + K_L g_{dl}^{-1}\theta_l(t) - K_L g r_{dl}^{-1} d_\alpha(t) \end{aligned} \tag{15}$$

$$\begin{aligned} J_l\ddot{\theta}_l(t) &= -c_l\dot{\theta}_l(t) - F_l \\ &\quad + K_L g_{dl}^{-1}\theta_d(t) - K_L\theta_l(t) + K_L d_\alpha(t). \end{aligned} \tag{16}$$

2.3 Friction Model

By the surface with which the object contact is not smooth, friction occurs. By considering the contact surface of the object as a collection of bristles, the LuGre model[2] is represented as the rigidity and viscosity of the bristles. In the model, this bristle is represented by a spring-damper system. The parameters of the LuGre model are shown in the Table 2.

Table 2 The parameters of the LuGre model

detail	charcters	unit
Displacement of bristles	z	[m]
Spring constant of bristle	σ_0	[N/m]
Damper constant of bristle	σ_1	[kg/s]
Stribeck velocity	v_s	[m/s]
Coulomb friction	F_c	[N]
Static friction	F_s	[N]

The friction F_L generated by the LuGre model is given by the following equation,

$$F_L = \sigma_0 z + \sigma_1\dot{z} + c_d\dot{\theta_d}. \tag{17}$$

Here, z is the displacement of the bristle and has the following dynamics,

$$\dot{z} = \dot{\theta_d} - \sigma_0\frac{|\dot{\theta_d}|}{g(\dot{\theta_d})}z \tag{18}$$

$$g(\dot{\theta_d}) = F_c + (F_s - F_c)e^{-|\frac{\dot{\theta_d}}{v_s}|}. \tag{19}$$

Here, $g(\dot{\theta_d})$ of Eq.(19) represents Coulomb friction and Stribeck effect. Since $c_d\dot{\theta_d}$ representing viscous friction of Eq.(17) is linear, it can be compensated by considering it as a linear controlled object model. Therefore, we consider only the term given by the following equation as the friction to be compensated,

$$F = \sigma_0 z + \sigma_1\dot{z}. \tag{20}$$

2.4 Validation of Linearized Friction Model

The LuGre model can express nonlinear friction. However, when adding it to the controller, nonlinearity becomes a problem. In this paper, we propose a method to generate z using first order lag of $\dot{\theta_d}$. From this, let us consider linearizing nonlinear friction and converting it into a linear control system design problem.

We assume that$\frac{|\dot{\theta_d}|}{g(\dot{\theta_d})}$ in Eq.(18) is constant. Then, the dynamics of$z$ becomes linear, which is a first order delay system. Assuming $\frac{|\dot{\theta_d}|}{v_s} >> 1$ in Eq.(19), $g(\dot{\theta_d})$is approximated as follows,

$$g(\dot{\theta_d}) \triangleq F_c. \tag{21}$$

Furthermore, $|\dot{\theta_d}|$ is given as the average speed which is measured when converging to the target value in the experiment. By this, Eq.(18) can be rewritten as follows,

$$\dot{z} = \dot{\theta_d} - \sigma_0\alpha z \tag{22}$$

$$\alpha = \frac{|\dot{\theta_d}|}{F_c}. \tag{23}$$

Thus,$\dot{z}$ can be represented by a linear system which is a first order delay one.

As a verification of this method, we compare the original LuGre model with the proposed method. Comparison verification was done by adding step inputs to both models. At that time we set the value of $|\dot{\theta}_d|$, $|\dot{\theta}_l|$ to $0.1012[\mathrm{rad/s}], 0.16548[\mathrm{rad/s}]$. The figure on the drive disc is shown in Figure 3, and the Load Disc figure is shown in Figure 4.

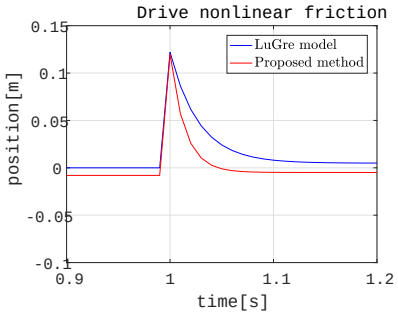

Figure 3 Drive Disc

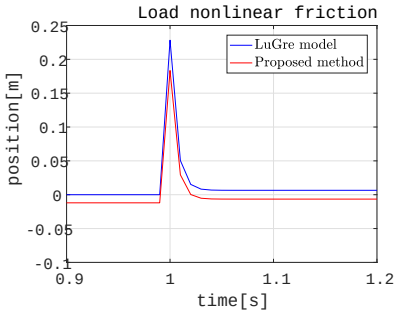

Figure 4 Load Disc

There are some errors in Figure 3, Figure 4, but they can be allowed.

3 CONTROL DESIGN

3.1 State Space Representation

State variable $x(t)$, input $u(t)$, and disturbance $w(t)$ are defined as follows,

$$x(t) = [\theta_d, \theta_l, \dot{\theta}_d, \dot{\theta}_l, z_d, z_l]^{\mathrm{T}}, u(t) = \tau, w(t) = d_\alpha(t).$$

the state space representation of the controlled object is given as follows,

$$\begin{cases} \dot{x}(t) = Ax(t) + B_1 w(t) + B_2 u(t) \\ y(t) = Cx(t) \end{cases} \tag{24}$$

$$A = \begin{bmatrix} 0 & 1 & 0 & 0 & 0 & 0 \\ -\frac{K_L g_{dl}^{-2}}{J_d^*} & -\frac{c_d}{J_d^*} & \frac{K_L g_{dl}^{-1}}{J_d^*} & 0 & 0 & 0 \\ 0 & 0 & 0 & 1 & 0 & 0 \\ \frac{K_L g_{dl}^{-1}}{J_l} & 0 & -\frac{K_L}{J_l} & -\frac{c_l}{J_l} & 0 & 0 \\ 0 & 1 & 0 & 0 & -\sigma_0\alpha & 0 \\ 0 & 0 & 0 & 1 & 0 & -\sigma_0\alpha \end{bmatrix}$$

$$B_1 = \begin{bmatrix} 0 \\ \frac{K_L g_{dl}^{-1}}{J_d^*} \\ 0 \\ \frac{K_L}{J_l} \\ 0 \\ 0 \end{bmatrix} \quad B_2 = \begin{bmatrix} 0 \\ \frac{1}{J_d^*} \\ 0 \\ 0 \\ 0 \\ 0 \end{bmatrix} \quad C = \begin{bmatrix} 0 & 0 & 1 & 0 & 0 & 0 \end{bmatrix}.$$

3.2 Servo System

In order to eliminate steady state error, we considered the servo system. Let $e(t)$ be the error between the output $y(t)$ and the reference $r(t)$. The state variables are redefined as follows,

$$x_e(t)^{\mathrm{T}} = [x(t) \int e(t)]^{\mathrm{T}}. \tag{25}$$

The servo system can be expressed as follows,

$$\dot{x_e}(t) = A_e x_e(t) + B_{1e} w(t) + B_{2e} u(t) \tag{26}$$
$$y(t) = C_1 x_e(t). \tag{27}$$

Here,the matrices$A_e, B_{1e}, B_{2e}, C_1, w(t)$ are as follows,

$$A_e = \begin{bmatrix} A & 0_{4\times1} \\ -C & 0 \end{bmatrix}, B_{1e} = \begin{bmatrix} B_1 & 0_{4\times1} \\ 0 & 1 \end{bmatrix},$$
$$B_{2e} = \begin{bmatrix} B_2 \\ 0 \end{bmatrix}, C_1 = \begin{bmatrix} C & 0 \end{bmatrix}, w(t) = \begin{bmatrix} d_\alpha \\ r \end{bmatrix}. \tag{28}$$

3.3 Matrix Polytopic Representation

In order to guarantee the robustness for the moment of inertia J_d^* and J_l which are uncertain parameters, they are specified as follows,

$$J_d^* \in [J_{d,min}^*, J_{d,max}^*] = [4.0 \times 10^{-4}, 9.8 \times 10^{-4}] \tag{29}$$
$$J_l \in [J_{l,min}, J_{l,max}] = [6.5 \times 10^{-3}, 8.5 \times 10^{-3}]. \tag{30}$$

Based on Eq.(29), Eq.(30), we considered the pattern of four endpoints as follows,

$$\{J_{d,min}^*, J_{l,min}\}, \{J_{d,max}^*, J_{l,min}\}$$
$$\{J_{d,min}^*, J_{l,max}\}, \{J_{d,max}^*, J_{l,max}\}. \tag{31}$$

For using polytopic representation, the end points of the variation range of matrices A_{ei}, B_{1ei}, B_{2ei} are given as follows,

$$A_{ei}(i = 1, 2, 3, 4),$$
$$B_{1ei} = (i = 1, 2, 3, 4), B_{2ei}(i = 1, 2, 3, 4).$$

If the system is stabilized at each endpoint of J_d^* and J_l, it may be said that the system is stabilized for all J_d^* and J_l.

3.4 H_∞Control

From the Eq.(24), the system of H_∞ control is defined as follows,

$$\begin{cases} \dot{x}_e(t) = A_e x_e(t) + B_{1e} w(t) + B_{2e} u(t) \\ z(t) = C_2 x_e(t) + D_2 u(t) \end{cases} \tag{32}$$

$$C_2 = \begin{bmatrix} W_e & 0_{6\times1} \\ 0 & W_e \\ 0 & 0 \end{bmatrix}, D_2 = \begin{bmatrix} 0_{6\times1} \\ 0 \\ W_u \end{bmatrix}. \tag{33}$$

Where, $z(t)$ is cost function. Let $W_x \succ 0, W_e \succ 0, W_u \succ 0$ are weight matrices for the state variable, integral and input. For the controller, let us consider to minimize H_∞ norm from disturbance $w(t)$ to the cost function $z(t)$. Here, the H_∞ norm is defined as follows,

$$||G_{zw}(s)||_\infty = \sup \frac{||z(t)||_2}{||w(t)||_2}. \tag{34}$$

If there exist $||G_{zw}(s)||_\infty \prec \gamma_\infty$, it is possible to guarantee the effect of suppressing the disturbance against the worst disturbance.

Variable conversion is performed and formulation of LMI condition is shown as follows,

$$
\begin{aligned}
&minimize : \gamma_\infty \\
&subject\ to X \succ 0 \\
&\begin{bmatrix} XA_{ei}^{\mathrm{T}} + A_{ei}X + B_{2ei}Y + Y^{\mathrm{T}}B_{2ei}^{\mathrm{T}} & * & * \\ C_2X + D_2Y & -\gamma_\infty I & 0 \\ B_{1ei}^{\mathrm{T}} & 0 & -\gamma_\infty I \end{bmatrix} \succ 0. \\
&\qquad\qquad\qquad\qquad\qquad\qquad\qquad\qquad (i = 1, 2, 3, 4) \\
&\qquad\qquad\qquad\qquad\qquad\qquad\qquad\qquad (35)
\end{aligned}
$$

At this time, when X and Y exist to staisfy the LMI expression (35),the system is stabilized by $u(t) = Kx_e(t) = YX^{-1}x_e(t)$.

4 SIMULATION

We performe a simulation of prpposed method, robust LQ which does not consider backlash and friction and H_∞control considering only backlash. As a result of measuring the angle of backlash in the experimental machine, the value of backlash is obtained as $1.2[deg] := 0.021[\mathrm{rad}]$. We set to the load disk angle reference to $\frac{\pi}{2} = 1.571[\mathrm{rad}]$. The simulation results of the load disk angle, input,backlash angle ,and friction are shown in Figure 5-Figure 8 in condition that the moment of inertia of the load disk and drive disk are minimum.

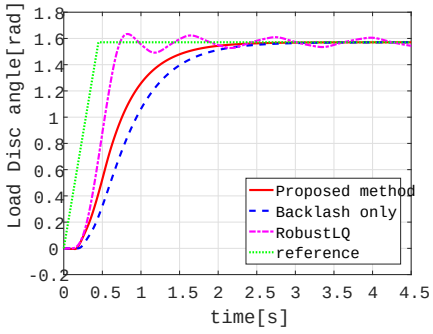

Figure 5 Load disc angle

From Figure 5-Figure 8, The angle of the load disk converged to the target value $\frac{\pi}{2}[\mathrm{rad}]$ asymptotically and earlier than the robust LQ control in the H_∞ control.

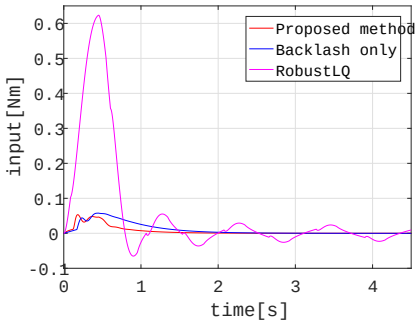

Figure 6 Input

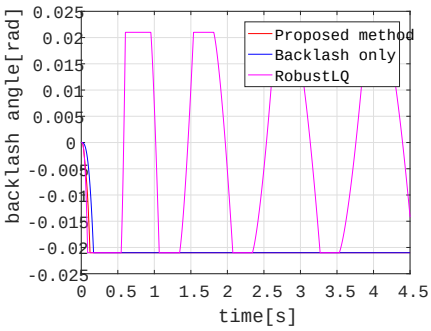

Figure 7 Backlash angle

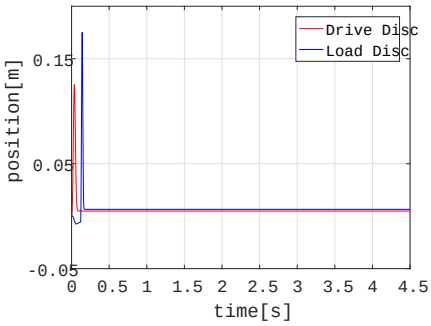

Figure 8 Friction

In addition, it was found possible to suppress the influence of the backlash that is treated as a disturbance. Friction occurs at start.

5 CONCLUSION

In this paper, in addition to the conventional model, LuGre model was used as modeling for friction. Moreover, by linearly approximating the LuGre model, its linearized model is derived. We treat the backlash as disturbance. The problem is formulated as a linear system control problem and H_∞ control. Theory is applied. The usefulness of the proposed method was verified by comparing simulation with robust LQ control which does not consider backlash and friction.

References

[1] L.Acho,F.Ikhouane,andG.Pujol: Robust Design for Mechanismes with Backlash, JCET, Vol.3, Iss.4, October 2013, pp.175-180.

[2] K. J. Astrom and C. Canudas de Wit: Revisiting the LuGre friction model, IEEE Control Systems Magazine, Institute of Electrical and Electronics Engineers, Vol. 28, No. 6, pp.101-114, 2008.

[3] Masatsugu HIBINO: H_∞control of Industrial Emulator with backlash,Graduate thesis of Mechatronics Graduate School of Science and Engineering Nanzan University, 2016.

[4] G.Pujol,L.Acho,: Stabilization of the Inverted Pendulum with backlash using H_∞-LMI Technique, Proceedings of the 17th World Congress The Internatinal Federation of Automatic Control Seoul, Korea, July 6-11, 2008.